Microbiome

RESEARCH

Open Access

An in vitro model demonstrating homeostatic interactions between reconstructed human gingiva and a saliva-derived multispecies biofilm

Lin Shang[1*], Sanne Roffel[2], Vera Slomka[3], Eleanor M. D'Agostino[3], Aline Metris[4], Mark J. Buijs[1], Bernd W. Brandt[1], Dongmei Deng[1], Susan Gibbs[2,5] and Bastiaan P. Krom[1]

Abstract

Background In the oral cavity, host-microbe interactions (HMI) continuously occur and greatly impact oral health. In contrast to the well-studied disease-associated HMI during, for example, periodontitis, HMI that are essential in maintaining oral health have been rarely investigated, especially in a human-relevant context. The aim of this study was to extensively characterize homeostatic HMI between saliva-derived biofilms and a reconstructed human gingiva (RHG). RHG was reconstructed following the structure of native gingiva, composed of a multilayered epithelium formed by keratinocytes and a fibroblast-populated compartment. To mimic the oral environment, RHG were inoculated with pooled human saliva resuspended in different saliva substitute media and incubated for 2 or 4 days. The co-cultured biofilms were retrieved and characterized by viable bacterial counting and compositional profiling (16S rRNA gene sequencing). RHG was investigated for metabolic activity (MTT assay), tissue histology (hematoxylin and eosin staining), epithelial proliferation (Ki67 staining), antimicrobial peptide expression, and cytokine secretion.

Results Viable biofilms were detected up to day 4 of co-culturing. Bacterial counts indicated biofilm growth from the inoculation to day 2 and maintained thereafter at a similar level until day 4. All biofilms shared similar composition throughout 4 days, independent of co-culture time and different saliva substitute media used during inoculation. Biofilms were diverse with *Streptococcus*, *Haemophilus*, and *Neisseria* being the dominating genera. While supporting biofilm development, RHG displayed no significant changes in metabolic activity, tissue histology, or epithelial proliferation. However, in the presence of biofilms, the antimicrobial peptides elafin and human β-defensin-2 were upregulated, and the secretion of cytokines IL-6, CXCL1, CXCL8, CCL5, and CCL20 increased.

Conclusion This model mimicked homeostatic HMI where a healthy gingiva supported a viable, diverse, and stable microbial community, incorporating bacterial genera found on native gingiva. The gingiva model maintained its tissue integrity and exerted protective responses in the presence of biofilms over time. This study adds to the evidence that shows the important role of the host in maintaining homeostatic HMI that are essential for oral health.

Keywords Host-microbe interactions, Gingiva, Organotypic model, Biofilms, 16S rRNA gene sequencing

*Correspondence:
Lin Shang
l.shang@amsterdamumc.nl
Full list of author information is available at the end of the article

Introduction

In the oral cavity, the gingiva hosts millions of microbes in the form of biofilms which are complex and dynamic microbial communities in terms of spatial structures and compositions. These communities continuously interact with the gingiva and influence oral health and disease: homeostatic host-microbe interactions (HMI) contribute to the maintenance of a healthy gingiva, while dysregulated HMI drive disease progression [1]. Several in vitro and animal models have been established to reveal how dysregulated HMI lead to the onset of inflammatory oral diseases, such as gingivitis and periodontitis, via the interplay between pathogenic biofilms and excessive inflammatory responses in the periodontium including gingiva [2–5]. In contrast, there is limited knowledge on how the gingival health is maintained by homeostatic HMI, largely due to the fact that such complex HMI between a multispecies oral biofilm and a healthy gingiva have been rarely modelled and characterized in a human-relevant context in vitro.

Indirect evidence from animal and in vitro models has indicated that HMI contribute to the maintenance of human oral health in various ways. For the host, constant microbial exposure is essential in maintaining a healthy gingiva [6]. Without the presence of resident oral microbiota, less neutrophil infiltration in the periodontium was found in germ-free mice than in specific-pathogen-free mice, due to defective chemoattractant signaling [7]. In addition, the oral microbiota induces and maintains the expression of various molecules in the host that benefit the gingival homeostasis, including antimicrobial peptides (AMP) and pro-inflammatory cytokines [8, 9]. For example, exposure to a commensal biofilm was associated with a high level of expression of growth arrest-specific 6 (GAS6) in the gingival epithelium in healthy wild-type mice, ensuring local homeostasis via the activation of TYRO3-AXL-MERTK (TAM) signaling. In contrast, GAS6-deficient mice presented a disturbed gingiva in terms of increased secretion of inflammatory cytokines, elevated frequencies of neutrophils, upregulated activity of enzymes, and imbalanced Th17/T_{reg} ratio [10]. Moreover, a stable microbial community, which is an essential part of homeostatic HMI, can also benefit oral health by allowing resident oral microbes to compete with potential pathogens, preventing them from overgrowing [3, 11]. Some microbial species have been individually identified for beneficial effects using co-culture models with monolayer host cells. The exposure to *Streptococcus gordonii* upregulated the expression of tight junction components in gingival epithelial cells, resulting in increased barrier function, as verified by decreased permeability to dextran [12, 13]. *Candida albicans* maintained a sufficient level of infiltrated IL-17-producing Th17 cells in gingiva in a murine model [14]. One important function of these Th17 cells, shown in a periodontitis mouse model, is to respond according to the pathogenicity of the biofilms, thereby contributing to mucosal homeostasis [15].

Nevertheless, the abovementioned evidence linking HMI to oral health is derived from animal or in vitro studies, which do not fully represent the human context in terms of the host physiology and the microbiome. Animal models are intrinsically different from humans in terms of tissue immunity and microbiome [16]. Conventional two-dimensional (2D) co-culture models, although consisting of relevant human cells and microbial species, lack the tissue mimicking the multicellular environment and spatial structure of the native gingiva. These models are also often limited by the use of single microbial species which cannot offer the functional diversity of the oral microbial community [17]. In addition, 2D models are not optimal for studying HMI with living microbes for longer than 24 h due to the significant difference in growth rate between eukaryotic and prokaryotic cells. On the other hand, clinical studies are the most realistic but are not practical for characterizing HMI. Such studies often require invasive methodologies, which are not applicable to healthy subjects due to the strict ethical regulations [17–19]. Therefore, to understand how HMI contribute to the maintenance of a healthy oral cavity, a relevant model, portraying the human situation, is needed for extensive characterization of both the host and the microbial community.

With the development of tissue engineering technologies, organotypic reconstructed human gingiva (RHG) models have been increasingly used and valued as a promising platform for studying (patho)physiology of the human gingiva and have application in safety assessment without the need for animal testing [19–21]. RHG consists of a stratified epithelium over a fibroblast-populated collagen hydrogel which serves as the *lamina propria*, mimicking the native gingiva in terms of the multicellular environment as well as the three-dimensional (3D) structure. Recent advances to increase their physiological relevance have further added elements to such models, e.g., saliva flow [22–24], teeth equivalents [25, 26], dental implants [27, 28], and immune cells [29, 30]. Also, living oral microbes and microbial components have been incorporated to mimic HMI (reviewed in [31, 32]). Nevertheless, most of the current oral HMI models have focused on understanding HMI that are associated with oral disease. They were inoculated with specific single species or selected multiple species (maximum 11) with known pathogenic characteristics (e.g., high invasiveness) to show how these specific pathogenic challenges lead to inflammatory responses and tissue disruption [17,

32]. Although in some studies selected oral commensal species to represent healthy HMI, e.g., *S. gordonii* [33] and *Streptococcus oralis* [34], have been used, there are currently very few studies that have modelled and further characterized the homeostatic HMI and their relationship with oral health.

Previously, in order to resemble the human oral HMI, we have developed a RHG model and exposed it to various microbial stimuli, from bacteria in single-species planktonic cultures [35, 36] to human saliva [37] or multispecies biofilms derived from human saliva with known compositions and phenotypes that represented commensal or pathogenic oral biofilms in vivo [38–41]. By using an optimized agar method, we even extended the co-culture period of RHG with living single-species bacteria to 5 days [36, 37]. In line with native gingiva, the RHG responded according to different types of microbial exposure by activating defense mechanisms while maintaining tissue integrity. However, it is yet to be extensively characterized, within the same model, how a dynamic balance is established and maintained by interactions between a multispecies microbial community and a RHG representing the healthy gingiva.

The aim of this study was to elucidate HMI between the RHG and multispecies biofilms for an extended co-culture period of up to 4 days, characterizing the co-development of biofilms and a healthy RHG in order to maintain homeostasis. Biofilms were evaluated for viability, species composition, and diversity to determine to what extent they represent a healthy gingival microbiome. To evaluate the host response to biofilm development, RHGs were assessed by tissue histology, metabolic activity, AMP expression, and cytokine secretion. Furthermore, three different saliva substitutes mimicking the moisturized salivary environment were incorporated in the model and compared in terms of their influence on the abovementioned HMI outcome.

Methods

Cell culture and RHG model

Two telomerase reverse transcriptase (TERT) immortalized human gingival cell lines were used to reconstruct RHG: keratinocytes (TERT-KC, OKG4/bmi1/TERT, Rheinwald Laboratory, Boston, MA, USA) and fibroblasts (TERT-Fib, T0026, ABM, Richmond, BC, Canada). TERT-KC were cultured at 37 °C and 7.5% CO_2 in KC medium consisting of DMEM/Ham's F-12 (3:1) (Gibco, Grand Island, NY, USA), supplemented with 5% FetalClone III (GE, Logan, UT, USA), 1% penicillin–streptomycin (Gibco), 1-μM hydrocortisone (Sigma-Aldrich, St. Louis, MO, USA), 0.1-μM insulin (Sigma-Aldrich, St. Louis, MO, USA), 1-μM isoproterenol (Sigma-Aldrich, St. Louis, MO, USA), and 2 ng/mL epidermal growth factor (EGF) (Sigma-Aldrich, St. Louis, MO, USA). TERT-Fib were cultured at 37 °C, 5% CO_2 in Fib medium consisting of DMEM with 5% FetalClone III and 1% penicillin–streptomycin.

RHG was constructed using TERT-KC and TERT-Fib following the previously established procedure [38]. In short, on day 1, TERT-Fib were mixed with a collagen hydrogel and transferred to transwell inserts (0.4-μm pores, Corning, NY, USA) in a 6-well plate. On day 2, TERT-KC were seeded on top of each fibroblast-populated hydrogel. On day 5, RHG was lifted to the air–liquid interface and cultured in differentiation medium for another 10 days to induce epithelial differentiation. Differentiation medium contained DMEM/Ham's F-12 (3:1), supplemented with 1% FetalClone III, 1% penicillin–streptomycin, 0.1-μM insulin, 2-μM hydrocortisone, 1-μM isoproterenol, 10-μM carnitine (Sigma-Aldrich, St. Louis, MO, USA), 10-mM L-serine (Sigma-Aldrich, St. Louis, MO, USA), 0.4-mM L-ascorbic acid (Sigma-Aldrich, St. Louis, MO, USA), and 2 ng/mL EGF (Sigma-Aldrich, St. Louis, MO, USA). Three days before inoculation, RHG was refreshed with the same differentiation medium but without penicillin–streptomycin and hydrocortisone. This medium (RHG_M) was used for subsequent medium refreshing in the HMI model, the agar model, and the Amsterdam Active Attachment model, as described below.

Saliva inoculum

Unstimulated saliva was collected from 10 donors who were self-reported systemically healthy, had no periodontal disease or active caries, and had not taken any antibiotics for at least 3 months [41]. The study was approved by the Medical Ethical Committee of the University Medical Center, Amsterdam UMC (document number 2011/236), with signed and informed consent from each donor. For saliva collection, the donor was asked to refrain from oral hygiene for 24 h and not to drink or eat for at least 2 h prior to donation. The collected saliva was pooled and mixed with 60% glycerol (ratio of 1:1), and aliquots were stored at − 80 °C. Before storage, a sample was taken to determine the total anaerobic viable bacterial cell counts. The total CFU count was used later for calculating the dilution of the inoculum to the designated CFU. This batch of pooled saliva was used as inoculum throughout this study.

Saliva substitutes

To mimic the moisturized environment where oral host-microbe interactions occur in vivo, three saliva substitute media were used as vehicle for inoculation: (1) buffered semi-defined McBain medium (MB) [42], containing 2.5 g/L mucin (Sigma-Aldrich, St. Louis, MO, USA),

1 g/L yeast extract (BD Diagnostic Systems, Sparks, MD, USA), 0.35 g/L NaCl, 0.2 g/L KCl, 0.2 g/L $CaCl_2$, 2 g/L Bacto Peptone (Difco, Detroit, MI, USA), 2 g/L trypticase peptone (BBL, Cockeysville, MD, USA), 0.1 g/L cysteine hydrochloride, 1 mg/L hemin (Sigma-Aldrich, St. Louis, MO, USA), 0.2 mg/L vitamin K1, 2 g/L sucrose, and 50-mM PIPES at pH = 7.0; (2) a self-defined artificial saliva medium (AS) mimicking saliva composition, containing 2.5 g/L mucin, 1 g/L yeast extract, 0.35 g/L NaCl, 0.2 g/L KCl, 0.1 g/L $CaCl_2$, 0.01 g/L $MgCl_2$, 0.33 g/L KH_2PO_4, 0.34 g/L Na_2HPO_4, 2.65 g/L NaH_2CO_3, 1 mg/L hemin, 0.2 mg/L vitamin K1, and 1 g/L glucose at pH = 7.0; and (3) filtered saliva with mucin (FSM): pooled human saliva filter-sterilized with a 0.2-μm filter (Sarstedt, Numbrecht, Germany), supplemented with 2.5 g/L mucin (Sigma-Aldrich, St. Louis, MO, USA).

HMI model

RHG was exposed to one of the following conditions: (1) unexposed; (2) MB, AS, or FSM in agar without inoculum; or (3) MB, AS, or FSM in agar with an inoculum of 10^4 colony-forming units (CFU)/culture: in detail, stored inocula were thawed on ice and centrifuged and diluted to the designated CFU using a freshly sterilized agar solution (BD Biosciences, CA, USA) supplemented with one of the three saliva substitutes (MB, AS,or FSM) at a 1:1 ratio to reach a final agar concentration of 0.3%. Then 50 μL of each agar solution was applied onto the center of RHG where it solidified immediately. Two samples of the used inocula were saved: one for sequencing and the other one was plated out on a tryptic soy-blood agar plate (TSBA, containing 5% sheep blood, 5 μg/mL hemin, and 1 μg/mL menadione) to confirm the initial CFU. The HMI models were further cultured at 37 °C, 7.5% CO_2, and 95% humidity with daily medium refreshments with RHG_M (differentiation medium without penicillin–streptomycin and hydrocortisone).

On day 2 and day 4, HMI models were harvested for the following: microbial viability (CFU), microbial community composition (16S rRNA gene sequencing), RHG metabolic activity (MTT assay), RHG tissue histology and in situ protein expression (immunohistochemical staining and fluorescence in situ hybridization (FISH)), and cytokine secretion (enzyme-linked immunosorbent assay (ELISA)). In addition, during harvesting, RHG culturing medium of each sample was plated out (100 μL) on a TSBA plate and incubated anaerobically for 5 days at 37 °C to check that it was free of contamination.

Agar model

Immediately after the inoculation procedure of the HMI model, 50-μL solution was taken from each inoculum (prepared in MB, AS, or FSM) and cultured in a sterile 24-well plate to determine the biofilm growth in the absence of RHG. In addition, the RHG-M medium was used to make the fourth condition where agar solution was prepared in the same way as other inocula. For each plate, half of the wells (12 wells) were used for the agar model, while the remaining 12 wells were filled with 2-mL phosphate-buffered saline (PBS) each to maintain a high environmental humidity in order to prevent the agar from drying out. The plate was then incubated for 2 or 4 days at 37 °C, 7.5% CO_2, and 95% humidity, similarly to the HMI model. For harvesting, agar biofilms were resuspended in 1 mL of PBS and collected. The samples were further dispersed using a sonicator with a maximum of 130 W and 20 kHz for 1 min with 40% amplitude and a pulse of 1 s (Vibra-Cell VCX130, Sonics & Materials, Newtown, CT, USA). Biofilm samples were serially diluted, plated on TSBA plates, and anaerobically cultured for 5 days at 37 °C, and biofilm formation was quantified by determining total viable bacterial cell counts.

Amsterdam Active Attachment (AAA) model

The AAA model was assembled with glass coverslips of diameter 12 mm (Menzel, Braunschweig, Germany) as previously described [42, 43]. A total of 1.5 mL/well of saliva inoculum from the same batch as used in the HMI and Agar models was diluted 1:50 in MB, AS, FSM, or RHG_M and inoculated in the AAA model. After inoculation, the AAA models were cultured for 6 h to allow active attachment of microbes to the coverslip and then refreshed with sterile media. The AAA models were cultured for either 2 or 4 days at 37 °C, 7.5% CO_2, and 95% humidity. For the 4-day condition, medium was refreshed again on day 2. Biofilms on the coverslips were harvested, sonicated, diluted, plated on TSBA plates, cultured anaerobically for 5 days, and assessed for viable bacterial cell counts.

Biofilm quantification of the HMI model

For the HMI model, half of each culture was mechanically homogenized in a glass tissue grinder and suspended and collected using 2-mL cysteine peptone water (CPW) containing 5 g/L yeast extract, 1 g/L peptone, 8.5 g/L NaCl, and 0.5 g/L L-cysteine hydrochloride (pH = 7.2). The 2-mL tissue homogenate was filtered through a 100-μm Falcon™ cell strainer (Corning, NY, USA) and serially diluted in CPW. The dilutions were plated on TSBA plates. The plates were incubated anaerobically for 5 days at 37 °C, and the colonies were counted to determine CFU. The remaining homogenates were centrifuged; supernatants were discarded, and pellets were stored at − 80 °C for DNA isolation.

16S rRNA gene sequencing and data analysis

Bacterial genomic DNA was extracted using phenol bead-beating and the Mag MiniKit as previously described (LGC Genomics, Berlin, Germany) [44, 45]. Bacterial pellets were mechanically disrupted in a lysis buffer with Tris-saturated phenol and zirconium beads. The DNA-containing phase was mixed with binding buffer and magnetic beads and then eluted. The DNA concentration was determined by qPCR and normalized to 2 ng per PCR reaction. The V4 region of the 16S rRNA gene was amplified with primers containing the respective Illumina adapters and a unique 8-nt index sequence key following the protocol established previously [46], except that 33 cycles were performed. The amplicon yields were determined with PicoGreen assay (Quant-iT™ PicoGreen™, Thermo Fisher Sci.) and equimolarly pooled into the amplicon pool. The pool was run on an agarose gel and purified. Paired-end sequencing of the purified amplicons was conducted for 2×251 nt on the MiSeq platform using MiSeq reagent kit v3 (Illumina, San Diego, CA, USA) at the Department of Clinical Genetics of Amsterdam University Medical Centre. The flow cell was loaded with 8-pmol DNA containing 30% PhiX.

The paired-end reads were merged, quality-filtered, and clustered into operational taxonomic units (OTUs) at 97% similarity. The most abundant sequence of each OTU was assigned to a taxonomy and classified using the Ribosomal Database Project (RDP) classifier and the Human Oral Microbiome Database version 14.51 [47], trimmed to the V4 region only [45]. The OTU table was subsampled at 19,000 reads per sample.

Taxonomic and principal compositional analysis (PCA) plots were created using the R (version 4.0.3) packages phyloseq (version 1.34.0) [48], microbiome (version 1.12.0), vegan (version 2.5–7), and ggplot2 (version 3.3.3). For the PCA plots, the OTU table was first log2-transformed to normalize the data distribution. Shannon index and observed OTU were generated using PAST (PAlaeontological STatistics version 4.03).

MTT assay

To determine the RHG metabolic activity, MTT assay was performed as previously described [38]. Briefly, a biopsy of 3-mm diameter was taken, incubated in a 2 mg/mL MTT solution (Sigma-Aldrich) for 2 h and then transferred to 200 µL of acidified isopropanol. After 24 h, absorbance was determined at 570 nm.

(Immuno)histochemistry and FISH

A strip from the central region of the HMI co-culture was fixed in 4% paraformaldehyde and embedded in paraffin. Tissue sections (5 µm) were cut and stained with hematoxylin and eosin (H&E) for histological analysis or used for immunohistochemistry with antibodies against Ki-67 (Dako, Agilent, USA), elafin (Hycult Biotech, The Netherlands), and human β-defensin 2 (hBD2) (OriGene Technologies, Rockville, USA), as previously described [41, 49]. Images were acquired using Nikon Eclipse 80i microscope (Nikon, Instruments Inc., Melville, USA) with 20×/0.50 and 40×/0.75 objectives.

FISH was performed on paraffin sections (All bacteria probe 10MEH000, Ribo Technologies, Groningen, The Netherlands). The sections were further counterstained and sealed using Fluoroshield mounting medium with DAPI (ab104139, Abcam, UK). Images were acquired using a TCS SP8 STED 3×confocal microscope (Leica Microsystems B.V., Wetzlar, Germany) with a 63×oil-immersion lens.

ELISA

Co-culture medium supernatant was collected daily, and cytokine release was assessed by ELISA as previously described [50]. IL-6, CXCL1, CCL5, and CCL20 antibodies and recombinant proteins were purchased from R&D Systems (Minneapolis, MN, USA). CXCL8/IL-8 was quantified using a human IL-8 ELISA kit (Diaclone, Besançon cedex, France).

Statistical analysis

For comparing the RHG metabolic activity after different co-culture conditions, two-way ANOVA was conducted for each time point using GraphPad Prism (version 9). To compare biofilms in terms of the microbial composition, permutational multivariate analysis of variance (PERMANOVA) was performed in PAST using the log2-transformed OTU table. Pairwise comparisons were conducted based on the Bray–Curtis similarity index and 9999 permutations. To determine bacterial taxa that differed among biofilms, Linear discriminant analysis Effect Size (LEfSe) [51] was performed using the log2-transformed table (one against all; alpha values of 0.05; https://huttenhower.sph.harvard.edu/galaxy/). LDA threshold was set to 2.5 when the inocula were excluded and to 3.5 when included. To compare the number of observed OTUs, Shannon index and the numbers of specific OTUs detected by LEfSe and one-way ANOVA were performed in GraphPad Prism. $P < 0.05$ was considered as significant. The P-values are denoted in figures as follows: $^{*}P < 0.05$, $^{**}P < 0.01$, $^{***}P < 0.001$, and $^{****}P < 0.0001$.

Results

HMI model supports biofilm development while maintaining tissue integrity

To determine whether the RHG was capable of supporting biofilm development in vitro, it was first compared with two other standard biofilm-culturing models in

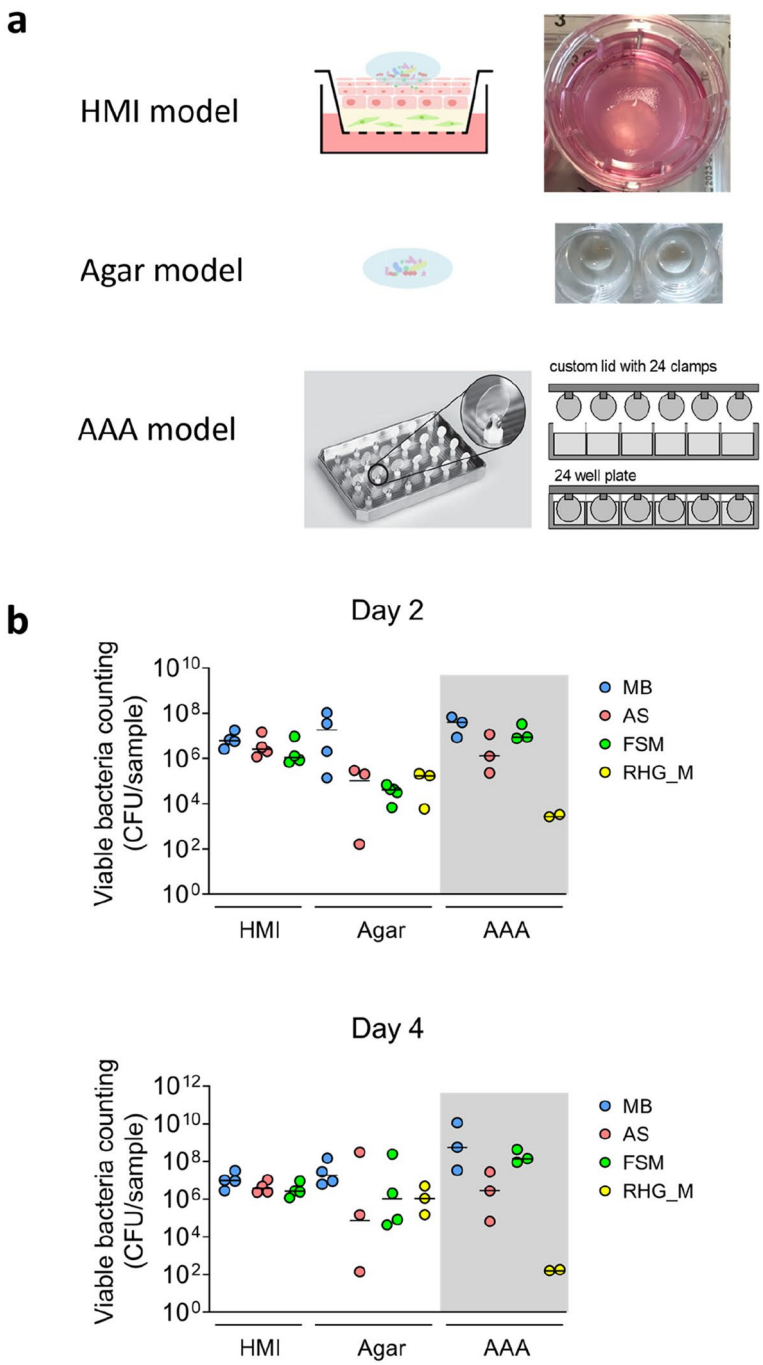

Fig. 1 Comparison of three in vitro biofilm-culturing models. **a** Setup of the three *in vitro* biofilm-culturing models. **b** Viable counts of bacteria derived from the same saliva inoculum after 2 or 4 days in each model. Counts of the AAA model are marked with a gray background as HMI and agar models were inoculated with similar bacterial amount (approximately 10^4), while AAA model was inoculated using a different procedure (details are described in the "Methods" and in [42, 43]). Each symbol represents the mean of two replicates from one independent experiment. The lines represent the average of at least three independent experiments per condition. AAA, Amsterdam Active Attachment model; MB, McBain medium; AS, artificial saliva medium; FSM, filtered saliva plus mucin medium; RHG_M, RHG differentiation medium without penicillin-streptomycin and hydrocortisone

which RHG was not present: the agar model (agar) and the AAA model (Fig. 1a, for details, see the "Methods"). The three models were inoculated with the saliva inoculum prepared in one of the saliva substitute media (MB, AS, or FSM) and then cultured for 2 or 4 days in the same environmental conditions. Since the HMI model was cultured in transwell inserts and had contact with the RHG differentiation medium from underneath, this medium (RHG_M) was also included in the agar and AAA model. Viable bacterial cell counts on day 2 and day 4 indicate that all three models supported growth of saliva-derived biofilms (Fig. 1b). Notably, the HMI model supported bacterial growth with the least variance, independent of the co-culture times or saliva substitute media. In the agar model, bacterial growth varied greatly depending on the type of saliva substitute media. In the AAA model, all three saliva substitute media supported bacterial growth however with more variance than those in the HMI model. The use of RHG_M medium in the AAA model consistently resulted in lower CFU counts on day 2 (4-log reduction) and day 4 (5–6 log reduction) when compared to all saliva substitute media. Notably, when comparing the four types of media, the use of MB resulted in a slightly higher bacterial growth compared to AS, FSM, and RHG_M in all three models.

Next, it was determined whether the biofilms influenced RHG tissue integrity by assessing metabolic activity, histology, and proliferation (Fig. 2). In general, RHG were not affected by the different experimental conditions: the presence or absence of biofilms (biofilm (−) or (+)), the co-culture time (days 2 or 4), or the use of different saliva substitute media (unexposed *versus* MB, AS, or FSM). Throughout the 4-day co-culture period, RHG co-cultured with or without biofilm showed a stable metabolic activity (Fig. 2a). All RHG, in the presence or absence of biofilms, showed similar tissue histology and proliferation with a stratified and differentiated epithelium on top of fibroblast-populated hydrogel representing the *lamina propria*, in line with the native human gingiva (as shown by H&E staining in Fig. 2b). In addition, all RHG had a similar number of proliferating Ki67-positive cells distributed throughout the basal layer of the epithelium (Fig. 2b).

Characterization of biofilms grown in the HMI model

Since the HMI model provides a unique opportunity to investigate biofilm development on RHG representing the healthy human gingiva, we next characterized these biofilms in further detail. HMI models were harvested and processed for (i) biofilm visualization using FISH (Fig. 3a), (ii) quantification of viable bacteria in the biofilm (Fig. 3b), and (iii) compositional analysis by means of 16S rRNA gene sequencing (Fig. 3c). Figure 3a shows clear visualization of biofilms on the surface of RHG via FISH. Viable bacterial counts were analyzed after 2 and 4 days of co-culturing and compared to the inoculum (approximately 10^4 CFU/culture, Fig. 3b, group Ino). Bacterial viability was not significantly affected by the use of different saliva substitute media. All CFU counts increased by 3-log on day 2 and remained at this level until day 4. Little variation was observed within the replicates of the groups. No detectable bacterial counts were detected in unexposed RHG and RHG co-cultured with saliva substitutes without biofilms on day 2 and day 4. This indicates that no contamination occurred during the 4 days of co-culturing in the absence of the traditionally used antibiotics, as well as during the sampling and processing for biofilm quantification.

Since viable biofilms were detected for up to 4 days of co-culture on RHG, we next extensively characterized their composition by sequencing the saliva inocula and day 2 and day 4 HMI biofilms. Sequencing data were first cross-checked between the experimental conditions and the acquired reads. From the 75 samples of biofilm-negative conditions (unexposed RHG and RHG exposed to saliva substitutes only), only two samples were found predominated by a single genus (one sample being *Streptococcus* and the other sample *Pseudomonas*) and were therefore considered contaminated and excluded from all analysis. The taxonomic plot illustrates the most abundant genera of all the sequenced samples (saliva inocula and HMI biofilms): 11 genera or higher taxa were identified with more than 1% relative abundance (Fig. 3c). The two types of biofilms, i.e., the saliva inocula (Ino) and the HMI biofilms, showed different diversity. While the inocula were predominated by the genera *Streptococcus*, *Prevotella*, *Veillonella*, *Haemophilus*, and *Neisseria*, the HMI biofilms were predominated by the genera *Streptococcus*, *Haemophilus*, and *Neisseria* despite the different co-culture periods (days 2 or 4) or different saliva substitute media conditions (MB, AS, or FSM).

When saliva inocula were excluded from the analyses and only HMI biofilm samples were analyzed for relative abundance, 9 of the 11 genera or higher taxa were identified with more than or equal to 1% relative abundance: *Neisseria*, *Haemophilus*, *Streptococcus*, *Rothia*, *Abiotrophia*, *Actinomyces*, *Capnocytophaga*, *Granulicatella*, and an unclassified order from family Neisseriaceae, while *Veillonella* and *Prevotella* were detected at less than 1% (data not shown).

The composition of biofilms on RHG is not affected by time or saliva substitute media

To determine what influenced and defined the composition of the HMI biofilms, bioinformatic and statistical analyses were performed. In line with the biofilm

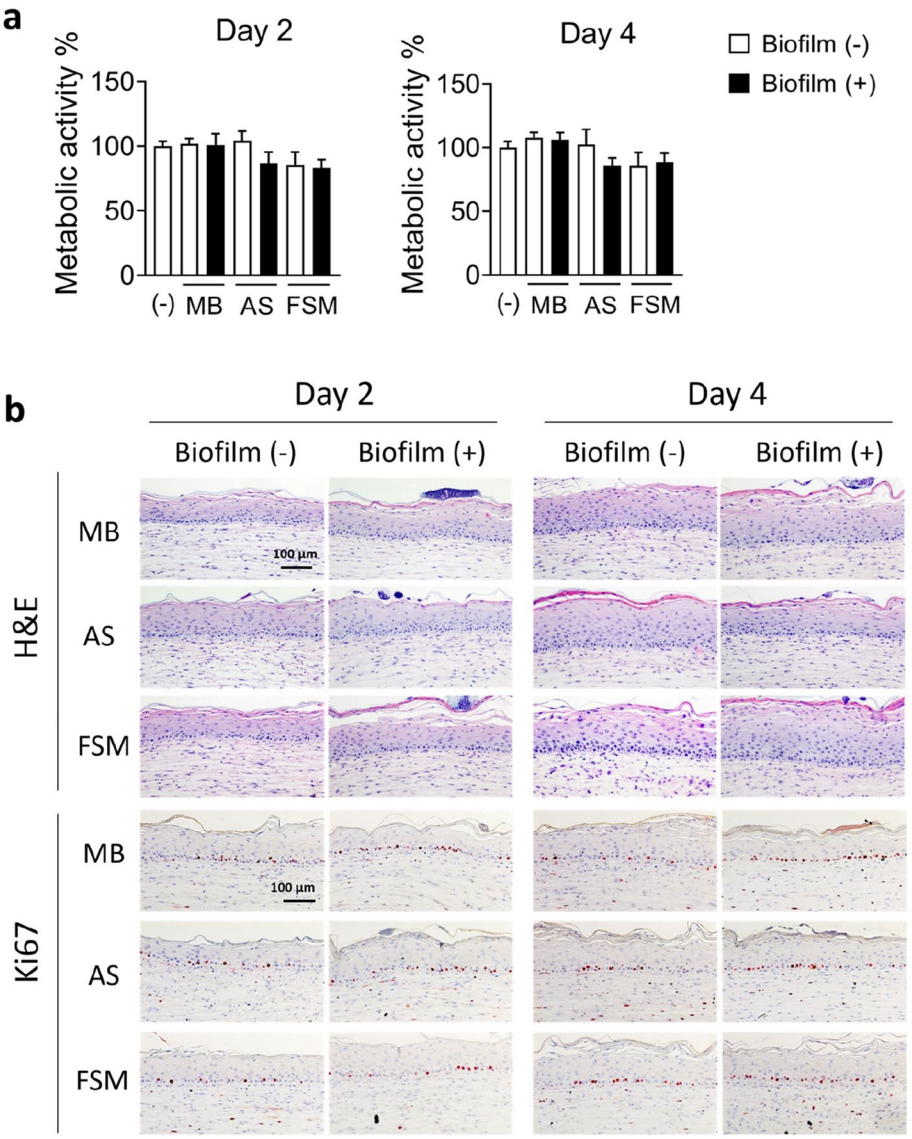

Fig. 2 Metabolic activity, tissue histology, and proliferation of RHG in the HMI model. **a** Metabolic activity of RHG on day 2 and day 4. All values are calculated relatively to the unexposed condition, shown as the first white bar (-) in both graphs. The rest of the white bars in each graph, labelled as biofilm (–), were conditions only exposed to agar supplemented with corresponding media. Data are shown as the mean ± SEM from four independent experiments, each performed in duplicate. **b** Hematoxylin and eosin (H&E) and Ki67 staining of RHG in the HMI model for 2 or 4 days. The photos represent the average of at least three independent experiments per condition. (-), unexposed; MB, McBain medium; AS, artificial saliva medium; FSM, filtered saliva plus mucin medium

composition illustrated in Fig. 3c, the observed OTU number and Shannon index indicated a significant difference between the inoculum and HMI biofilms, while no differences could be observed between HMI biofilms of different co-culture times or saliva substitute media (Fig. 4a). Similarly, the PCA plot showed two distant clusters representing the Ino and the HMI biofilms (Fig. 4b). Two sub-clusters of the HMI biofilms were seen on the right side of PC1 due to intra-experimental difference. These PCA-derived observations were supported by permutational multivariate analysis of variance (two-way PERMANOVA, $F=0.2925$, $P=0.6889$). The pairwise comparison confirmed that the HMI biofilms were significantly different from the saliva inocula. In contrast, HMI biofilms did not differ significantly from each other (Table 1).

To further understand which genera were different depending on the conditions, LEfSe analysis was performed, and the top 8 OTUs that differed the most based on LDA score are shown in Fig. 4c. The relative

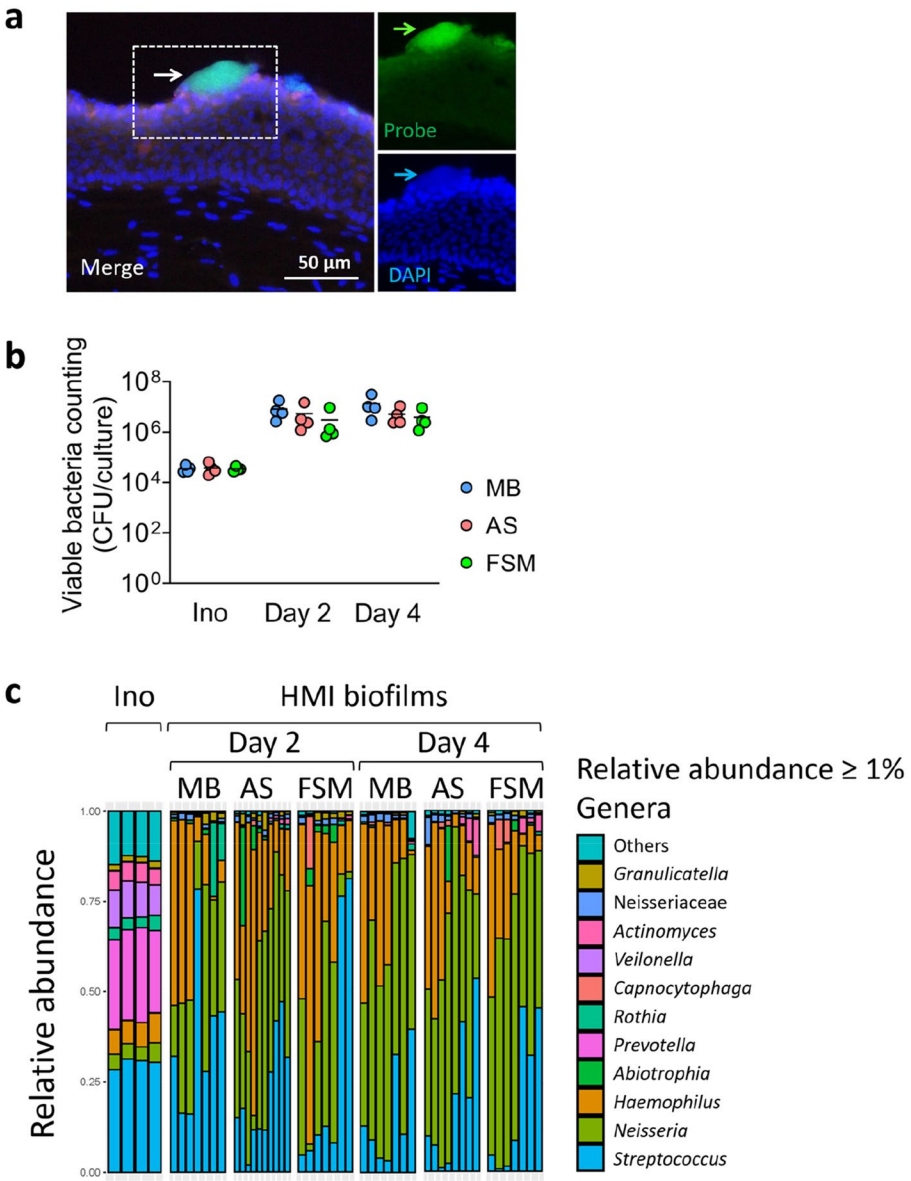

Fig. 3 Characterization of the HMI biofilms. **a** Representative FISH staining shows the presence of biofilms on RHG on day 2 (16S probe for all bacteria in green, DAPI in blue). **b** Viable bacterial counting of saliva inocula (Ino) and HMI biofilms on day 2 and day 4. Each symbol represents the count of inocula or the mean of two replicates of HMI biofilms from one independent experiment. **c** Relative abundance of major bacterial genera or higher taxa in the pooled data of saliva inocula (Ino) and HMI biofilms (day 2 and day 4). Eleven genera were identified at a relative abundance higher than 1% in any of the samples. The remaining 101 low abundance taxa are shown as one group (others). *MB*, McBain medium; AS, artificial saliva medium; FSM, filtered saliva plus mucin medium

abundance of OTU10 (*Prevotella*), OTU12 (*Rothia*), OTU22 (*Gemella*), and OTU17 (*Porphyromonas*) was significantly lower in all HMI biofilms than in the inoculum. The three predominating genera in HMI biofilms (*Neisseria*, *Haemophilus*, and *Streptococcus*) were all detected by LEfSe among the most differing OTUs. Only *Neisseria* (OTU2) showed statistically significant increase on day 4.

RHG-protective responses contribute to the maintenance of HMI

Next, we investigated the ability of RHG in conducting protective responses which are known to be essential for the healthy gingiva to maintain homeostasis with resident microbes as well as to prevent invasion of potential pathogens (e.g., expressing AMP and producing cytokines). The representative pictures of immunohistochemical

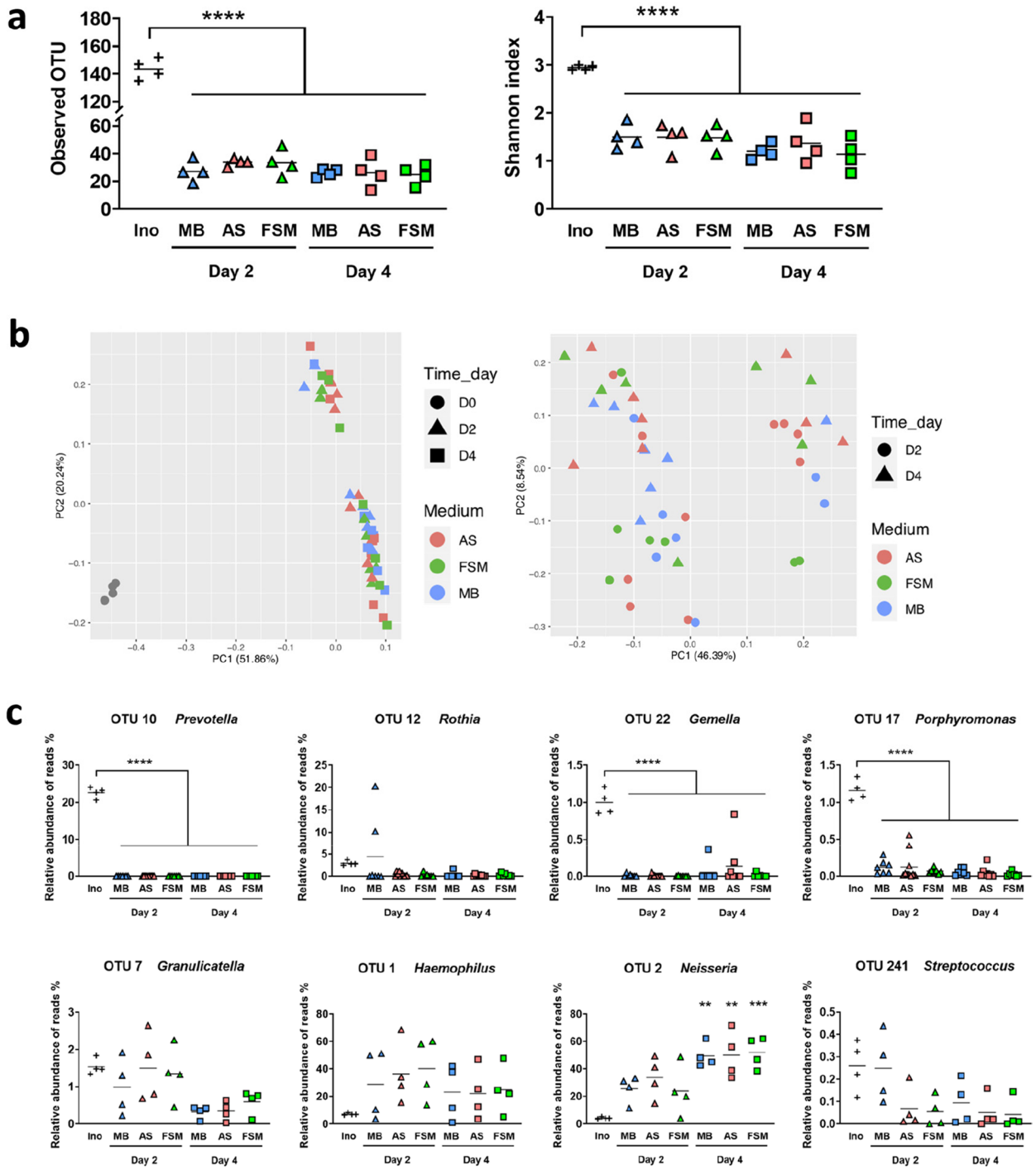

Fig. 4 The influence of different conditions on the HMI biofilm profiles. **a** Number of observed OTUs and Shannon index in all conditions. **b** Principal component analysis plots of microbial samples including saliva inocula (left) or excluding saliva inocula (right, only HMI biofilms). **c** OTUs that differentiated the most among all microbial samples ranked by LEfSe. Data are collected from four independent experiments, each performed in duplicate per condition. *Represents statistically significant difference between Ino and HMI biofilms. $^{**}P < 0.01$, $^{***}P < 0.001$, $^{****}P < 0.0001$. Ino, saliva inocula; MB, McBain medium; AS, artificial saliva medium; FSM, filtered saliva plus mucin medium

Table 1 Pairwise comparison of biofilms by one-way PERMANOVA analysis with Bonferroni correction

Biofilm	Ino	D2_MB	D2_AS	D2_FSM	D4_MB	D4_AS	D4_FSM
Ino		0.0186*	0.0090*	0.0192*	0.0036*	0.0018*	0.0024*
D2_MB	35.2600		1.0000	1.0000	0.3954	1.0000	1.0000
D2_AS	37.0800	0.7815		1.0000	1.0000	0.8759	1.0000
D2_FSM	29.6500	0.9832	0.7917		1.0000	1.0000	0.3336
D4_MB	24.3800	0.9613	0.5191	1.0310		1.0000	1.0000
D4_AS	34.3100	0.9546	0.4145	0.6372	0.9941		1.0000
D4_FSM	22.7600	0.9924	0.7016	1.0890	0.9680	0.9924	

P-values and *F*-values (gray background) are calculated using the Bray–Curtis distance and 9999 permutations

Ino saliva inocula, *MB* McBain medium, *AS* artificial saliva medium, *FSM* filtered saliva plus mucin medium

* Marks statistically significant difference ($P < 0.05$)

staining indicated increased expressions of two AMP (Elafin and hBD2) in the epithelium of RHG exposed to the biofilms, in comparison with the no biofilm-exposed RHG (biofilm (−) vs. biofilm (+), Fig. 5). This increase in AMP expression was observed in all biofilm-exposed RHG regardless of the type of saliva substitute media used or co-culture time.

Inflammatory cytokine secretion also showed an increase over time after biofilm exposure (Fig. 6). IL-6 secretion was significantly upregulated, while CXCL1, CXCL8, CCL5, and CCL20 secretion showed moderate increasing trends in the biofilm-exposed RHG compared with RHG cultured without biofilms. As seen before, the use of different saliva substitute media for the inoculation did not influence cytokine secretion throughout the 4 days of co-culturing.

Discussion

In this study, we established an in vitro oral HMI model that allowed a 4-day host-microbe co-culturing and an extensive profiling of both the biofilms and the host afterwards. This physiologically relevant model demonstrated a homeostatic and stable HMI between viable biofilms and a responsive gingiva for up to 4 days.

Our study focused on characterizing the biofilms which were co-cultured in vitro with the host RHG, in order to identify potential correlation of in vitro-generated data to the healthy in vivo situation. One important parameter is the maintenance of microbial viability. While microbial viability can be determined in 2D HMI models by collecting supernatants that contain living microbes, retrieving microbes from 3D HMI models can be more challenging due to the 3D construction as well as the limited amount of co-culture tissues. In some studies, samples for the determination of microbial viability were successfully recovered with the help of using tissue dissociators [39], homogenizers [52, 53], and osmotic lysing and scraping [53] or by implementing a removable insert for applying as well as harvesting microbes [54]. Alternatively, the morphology of biofilms in situ was assessed by visualization instead of determining the viability (reviewed in [32]). Pinnock et al. showed that by exposing a 3D oral mucosa directly to *Porphyromonas gingivalis*, the viability of internalized *P. gingivalis* decreased in a time-dependent manner to 0.001% after 48 h, compared to the initial inoculum [53]. De Ryck et al. successfully maintained the level of viable microbial cells for 72 h by creating an indirect host-microbe contact [54]. In our previous studies, we first applied saliva-derived biofilms in suspension on the surface of a 3D gingiva model and detected a 6-log decrease in microbial viability after 24 h. This substantial decrease was probably due to the presence of antibiotics in culture media underneath the gingiva model to avoid contamination [39]. Using a further developed agar method to inoculate the RHG with saliva inoculum, we managed to maintain the bacterial viability for 5 days without the presence of antibiotics [36, 37]. This method was therefore used in this study to ensure sufficient biofilm viability over time and to avoid potential contamination.

These viable biofilms were further characterized to understand the HMI in this model. Compositional analysis of the biofilms showed diverse communities which were predominated by *Streptococcus*, *Haemophilus*, and

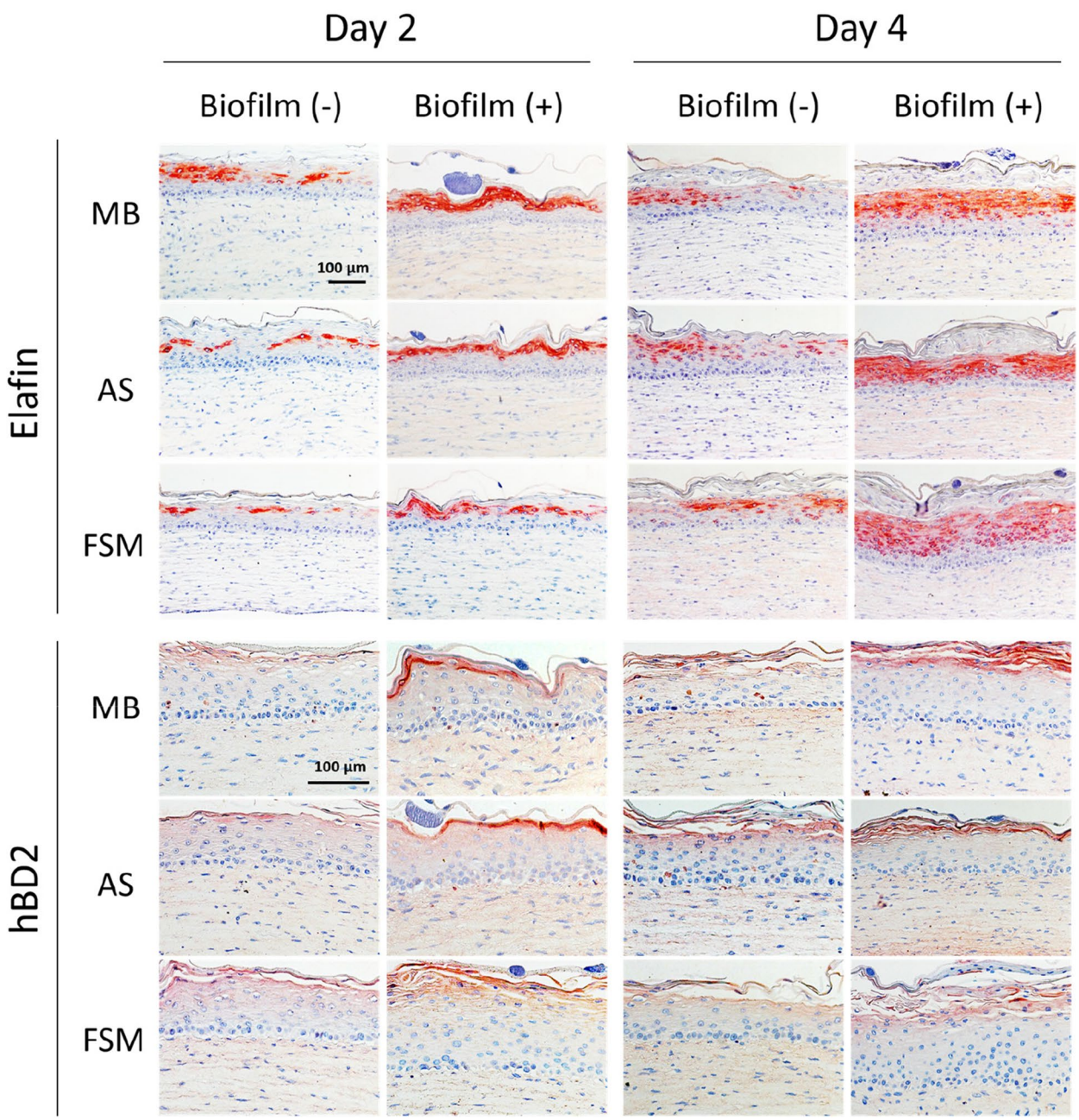

Fig. 5 Immunohistochemical staining of RHG in the HMI model. Expression of elafin and hBD2 in RHG co-cultured with (+) or without (–) biofilms for 2 or 4 days. Representative staining pictures are shown, from four independent experiments, each with an intra-experimental replicate. Biofilm (–), biofilm-negative condition; biofilm (+), biofilm-positive condition; MB, McBain medium; AS, artificial saliva medium; FSM, filtered saliva plus mucin medium

Neisseria. Of the nine top abundant genera preserved in the HMI model, six are identified as major colonizing genera on healthy gingiva in vivo [55, 56]. In comparison with the saliva inocula used in this study, the HMI biofilm was significantly less diverse. Of note, genera *Prevotella*, *Gemella*, and *Porphyromonas* decreased after they were introduced to the HMI model, which requires additional testing in order to have more clarity on the reason behind. However, the major genera of the saliva inocula were still remarkably preserved in our model, confirmed by the fact that 9 out of 11 dominating genera of the saliva inocula were retained and predominant in the HMI biofilms after even 4 days. These findings are in line with our previous study showing

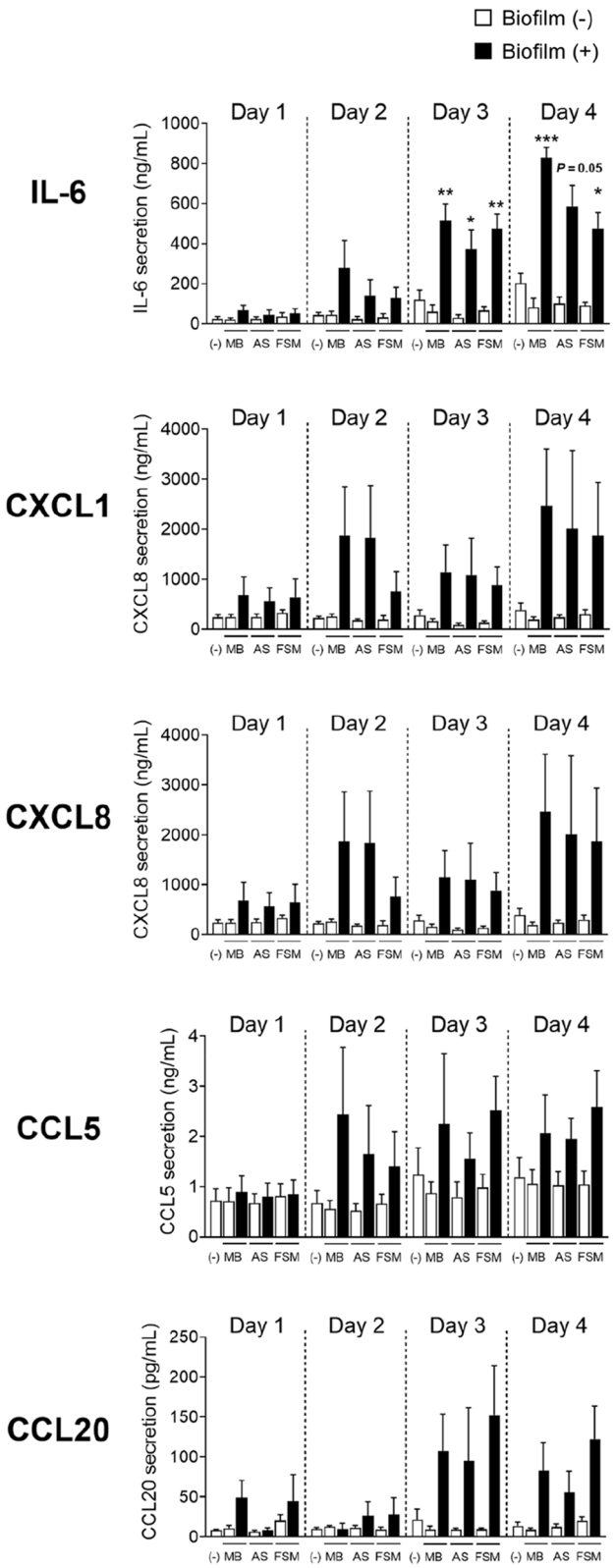

Fig. 6 Cytokine secretion of RHG in the HMI model. After exposing RHG to different biofilm conditions, cultures were refreshed with new medium every 24 h, and culture supernatants were collected and used to assess secretion of IL-6, CXCL1, CXCL8, CCL5, and CCL20 by means of ELISA. The unexposed condition is shown as the first white bar (-) in all graphs. The rest of the white bars in each graph, labelled as biofilm (–), were conditions only exposed to agar supplemented with corresponding media. Data represent the mean± SEM from four independent experiments, each performed in duplicate. Differences were considered significant when $P < 0.05$. *Represents statistically significant difference between one biofilm-positive condition and its corresponding biofilm-negative condition with the same saliva substitute. *$P < 0.05$; **$P < 0.01$; ***$P < 0.001$. Biofilm (–), biofilm-negative conditions; biofilm (+), biofilm positive conditions; (-), unexposed; MB, McBain medium; AS, artificial saliva medium; FSM, filtered saliva plus mucin medium

that RHG supported the diversity of saliva-derived biofilms better than two other inorganic substrates in vitro [37]. In that study, we were able to preserve five of the nine most abundant genera of the saliva inoculum from a single donor in the in vitro biofilms co-cultured with RHG for 1, 3, or 5 days [37]. The decreased diversity is foreseeable as the growth environment changed greatly from in vivo (saliva of healthy subjects) to in vitro (biofilms co-cultured with RHG at 37 °C, 95% humidity, and 7.5% CO_2). This change of environment was also reflected by the finding that the most differing genera between the inocula and the HMI biofilms were strict anaerobes (e.g., *Prevotella*, *Gemella*, and *Porphyromonas*), the abundance of which decreased significantly upon their co-culturing with the RHG in the aerobic co-culture environment. In comparison, aerobes and facultative anaerobes that can survive and thrive in this co-culture environment took dominance and have contributed the most to the increased viable bacterial counts. In a comparable 3D HMI study where cheek swab samples were used as inocula, compositional analysis showed that the inocula contained only one dominant family Streptococcaceae (relative abundance about 95%) which continued to expand over the co-culturing with the submerged mucosa model to more than 99% abundance within 1 day and then decreased slightly to 94% after 2 days [54]. This indicated again that preserving the richness and diversity of clinical samples in vitro is very challenging. Even with advanced biofilm-culturing models, e.g., the AAA model, where hard discs are used to mimic the attachment and development of biofilms on teeth, only 16 genera showed a relative abundance of > 1% after 14 or 28 days of in vitro culturing [43, 44]. The AAA model supports growth of fastidious anaerobic bacteria (37 °C, 80% N_2, 10% CO_2, and 10% H_2) such as *Veillonella*, *Fusobacterium*, *Rothia*, and *Peptostreptococcus* [37, 41,

44]. The observation that *Rothia* was abundant in the AAA model while *Neisseria* and *Haemophilus* were abundant in this HMI model is consistent with the in vivo situation where niche- and substrate-specific associations have been identified, e.g., the presence of *Rothia* spp.in dental plaque and tongue dorsum and *Haemophilus* and *Neisseria* spp. on gingiva [55, 57, 58]. Taken together, our HMI model was shown to support a diverse biofilm growth and preserved microbial species and community profiles representing the in vivo microbiome on a healthy gingiva.

Another feature of the presented HMI model is that it indicated homeostatic HMI. Biofilms not only represent the healthy gingival microbiome, as mentioned earlier, but also trigger the host RHG to initiate protective mechanisms during an extended co-culture period of 4 days. More interestingly, we found that all biofilms developed on RHG had similar profiles which were independent of the use of different inoculation media, i.e., saliva substitutes and culture time (day 2 *versus* day 4). This implies the host's important role in maintaining oral homeostasis, which, to date, has been rarely demonstrated directly in vitro with extensive characterization on both the microbial community and the host at the same time. Considering different model setups may contribute greatly to the differentiating HMI outcomes [59], we have therefore focused on comparing the current study with other 3D models using single microbe species or synthetic biofilms and reconstructed gingiva models in vitro. A recent in vitro study suggested that the integrity of gingival epithelial barrier is one of the host's important protection mechanisms against *P. gingivalis* invasion and its LPS [60]. In comparison, many 3D oral HMI models have focused on elucidating how pathogenic biofilms damage the host and its defense by showing pathogen-caused tissue disruption, as indicated by increased lactate dehydrogenase (LDH) production and decreased metabolic activity [27, 61, 62]. In some of these models, nonpathogenic HMI conditions were included as controls and showed less tissue damage than the pathogenic HMI conditions. The microbial exposures used for these nonpathogenic conditions were as follows: (i) a saliva-derived commensal biofilm for 24 h [41] and 7 days [39], (ii) a buccal microbiome-derived biofilm for 24–72 h [54], (iii) a denture-associated 4-species biofilm for 12 h [62], (iv) a 7-species subgingival biofilm for 24 h [62], (v) a *S. gordonii* exposure for 72 h [36], and (vi) a saliva-derived biofilm for 5 days [37]. This is in line with our finding that the 4-day co-culturing with biofilms did not result in destructive changes in RHG morphology. In addition, the RHG maintained metabolic activity and clearly exerted protection in response to the living biofilms. The increased AMP expression and cytokine release are in agreement with the defensive strategies observed in native gingiva, which are continuously occurring in order to maintain the local homeostasis [6, 63, 64].

The present study still has limitations. The HMI model lacks important features that may have significant influence on HMI, such as the presence of immune cells. In the future, incorporation of neutrophils, macrophages, or antigen-presenting cells (APC) should be considered, as they are known to greatly contribute to gingival homeostasis [6, 17, 63]. While sub-types of immune cell have yet to be included in a 3D oral HMI model, their integration should be theoretically feasible based on relevant studies which have shown the possibility to include Langerhans cells, a type of APC, in an multi-organ model containing RHG and a reconstructed human skin [65, 66]. Furthermore, based on the niche-specificity theory [55], HMI may vary significantly per niche in the oral cavity, and therefore, it might be of interest to pair specific microbial exposure with matching host models, e.g., gingival microbiome-derived biofilms and RHG.

Conclusions

In this study, we presented an in vitro HMI model mimicking a homeostatic HMI where a healthy gingiva is competent in hosting viable, diverse, and representative oral biofilms for an extended period. We have shown in vitro the important role of the host in maintaining gingival homeostasis with a multispecies biofilm derived from human saliva.

Abbreviations

HMI	Host-microbe interactions
RHG	Reconstructed human gingiva
CFU	Colony-forming units
AAA	Amsterdam Active Attachment model
MB	McBain medium
AS	Artificial saliva medium
FSM	Filtered saliva plus mucin medium

Acknowledgements

We thank Unilever Oral Care and Unilever Safety and Environmental Assurance Centre (SEAC) for scientific and financial support. We thank Dr. Richard Skinner, Dr. Robert Marriott, and Dr. Ann Scott (Unilever Oral Care, Bebington, UK) for their critical evaluation of the manuscript. We thank Dr. Rob Exterkate and Dr. Marleen Janus for their help with the preparation of AAA model and saliva inocula.

Authors' contributions

Conception and design of this study: L.S., V.S., E.M.D'A., A.M., D.D., S.G. and B.P.K.. Laboratory experiments: L.S., S.R. and .M.J.B.. 16S rRNA gene sequencing process: M.J.B.. Bioinformatics processing: L.S. and B.W.B.. Data analysis and interpretation: L.S., S.R., V.S., E.M.D'A., A.M., B.W.B., D.D., S.G. and B.P.K.. Initial draft of the manuscript: L.S.. Major contributors to writing of the manuscript: L.S., D.D., S.G. and B.P.K.. Critical revision of the manuscript: L.S., V.S., A.M., B.W.B., D.D., S.G. and B.P.K.. All authors read and approved the final manuscript.

Funding

This study was funded by Unilever.

Data availability
Sequence data that support the findings of this study have been deposited in the NCBI Sequence Read Archive (SRA) database under accession number SUB14263490.

Declarations

Ethics approval and consent to participate
The study was approved by the Medical Ethical Committee of the University Medical Center, Amsterdam UMC (document number 2011/236) with signed and informed consent from each donor.

Consent for publication
Not applicable.

Competing interests
VS, AM and ED'A were Unilever employees at the time of the described work. The authors declare no competing interests.

Author details
[1]Department of Preventive Dentistry, Academic Centre for Dentistry Amsterdam (ACTA), University of Amsterdam and Vrije Universiteit Amsterdam, Amsterdam 1081 LA, The Netherlands. [2]Department of Oral Cell Biology, Academic Centre for Dentistry Amsterdam (ACTA), University of Amsterdam and Vrije Universiteit Amsterdam, Amsterdam, The Netherlands. [3]Unilever Oral Care, Bebington, UK. [4]Unilever Safety and Environmental Assurance Centre (SEAC), Colworth Science Park, Sharnbrook, Bedford, UK. [5]Department of Molecular Cell Biology and Immunology, Amsterdam University Medical Centre Location Vrije Universiteit Amsterdam, Amsterdam Infection and Immunity Institute, Amsterdam, The Netherlands.

Received: 12 September 2024 Accepted: 7 January 2025
Published online: 28 February 2025

References

1. Bowen WH, et al. Oral biofilms: pathogens, matrix, and polymicrobial interactions in microenvironments. Trends Microbiol. 2018;26(3):229–42.
2. Lamont RJ, Koo H, Hajishengallis G. The oral microbiota: dynamic communities and host interactions. Nat Rev Microbiol. 2018;16(12):745–59.
3. Valm AM. The structure of dental plaque microbial communities in the transition from health to dental caries and periodontal disease. J Mol Biol. 2019;431(16):2957–69.
4. Belstrom D. The salivary microbiota in health and disease. J Oral Microbiol. 2020;12(1):1723975.
5. Hajishengallis G. Periodontitis: from microbial immune subversion to systemic inflammation. Nat Rev Immunol. 2015;15(1):30–44.
6. Moutsopoulos NM, Konkel JE. Tissue-specific immunity at the oral mucosal barrier. Trends Immunol. 2018;39(4):276–87.
7. Zenobia C, et al. Commensal bacteria-dependent select expression of CXCL2 contributes to periodontal tissue homeostasis. Cell Microbiol. 2013;15(8):1419–26.
8. Vankeerberghen A, et al. Differential induction of human beta-defensin expression by periodontal commensals and pathogens in periodontal pocket epithelial cells. J Periodontol. 2005;76(8):1293–303.
9. Sancilio S, et al. Biological responses of human gingival fibroblasts (HGFs) in an innovative co-culture model with Streptococcus mitis to thermosets coated with a silver polysaccharide antimicrobial system. PLoS One. 2014;9(5): e96520.
10. Nassar M, et al. GAS6 is a key homeostatic immunological regulator of host-commensal interactions in the oral mucosa. Proc Natl Acad Sci U S A. 2017;114(3):E337–46.
11. Hanel AN, et al. Effects of oral commensal streptococci on Porphyromonas gingivalis invasion into oral epithelial cells. Dent J (Basel). 2020;8(2):39.
12. Ye P, et al. Binding of Streptococcus gordonii to oral epithelial monolayers increases paracellular barrier function. Microb Pathog. 2013;56:53–9.
13. Takahashi N, et al. Gingival epithelial barrier: regulation by beneficial and harmful microbes. Tissue Barriers. 2019;7(3): e1651158.
14. Kirchner FR, LeibundGut-Landmann S. Tissue-resident memory Th17 cells maintain stable fungal commensalism in the oral mucosa. Mucosal Immunol. 2021;14(2):455–67.
15. Dutzan N, et al. A dysbiotic microbiome triggers TH17 cells to mediate oral mucosal immunopathology in mice and humans. Sci Transl Med. 2018;10(463):eaat0797.
16. Moysidou CM, Owens RM. Advances in modelling the human microbiome-gut-brain axis in vitro. Biochem Soc Trans. 2021;49(1):187–201.
17. Mountcastle SE, et al. A review of co-culture models to study the oral microenvironment and disease. J Oral Microbiol. 2020;12(1): 1773122.
18. Barrila J, et al. Modeling host-pathogen interactions in the context of the microenvironment: three-dimensional cell culture comes of age. Infect Immun. 2018;86(11):e00282.
19. Bierbaumer L, et al. Cell culture models of oral mucosal barriers: a review with a focus on applications, culture conditions and barrier properties. Tissue Barriers. 2018;6(3): 1479568.
20. Métris A, et al. A tiered approach to risk assess microbiome perturbations induced by application of beauty and personal care products. Microbial Risk Anal. 2022;20:100188.
21. Gibbs S, et al. Biology of soft tissue repair: gingival epithelium in wound healing and attachment to the tooth and abutment surface. Eur Cell Mater. 2019;38:63–78.
22. Diaz PI, et al. Synergistic interaction between Candida albicans and commensal oral streptococci in a novel in vitro mucosal model. Infect Immun. 2012;80(2):620–32.
23. Bao K, et al. Proteomic profiling of host-biofilm interactions in an oral infection model resembling the periodontal pocket. Sci Rep. 2015;5:15999.
24. Bao K, et al. Establishment of an oral infection model resembling the periodontal pocket in a perfusion bioreactor system. Virulence. 2015;6(3):265–73.
25. Gursoy UK, et al. A novel organotypic dento-epithelial culture model: effect of Fusobacterium nucleatum biofilm on B-defensin-2, -3, and LL-37 expression. J Periodontol. 2012;83(2):242–7.
26. Pollanen MT, et al. Fusobacterium nucleatum biofilm induces epithelial migration in an organotypic model of dento-gingival junction. J Periodontol. 2012;83(10):1329–35.
27. Souza JGS, et al. Biofilm interactions of Candida albicans and mitis group streptococci in a titanium-mucosal interface model. Appl Environ Microbiol. 2020;86(9):e02950.
28. Ingendoh-Tsakmakidis A, et al. Commensal and pathogenic biofilms differently modulate peri-implant oral mucosa in an organotypic model. Cell Microbiol. 2019;21(10): e13078.
29. Schaller M, et al. Polymorphonuclear leukocytes (PMNs) induce protective Th1-type cytokine epithelial responses in an in vitro model of oral candidosis. Microbiology (Reading). 2004;150(Pt 9):2807–13.
30. Brown JL, et al. Biofilm-stimulated epithelium modulates the inflammatory responses in co-cultured immune cells. Sci Rep. 2019;9(1):15779.
31. Barrila J, et al. Organotypic 3D cell culture models: using the rotating wall vessel to study host-pathogen interactions. Nat Rev Microbiol. 2010;8(11):791–801.
32. Tabatabaei F, Moharamzadeh K, Tayebi L. Three-dimensional in vitro oral mucosa models of fungal and bacterial infections. Tissue Eng Part B Rev. 2020;26(5):443–60.
33. Dickinson BC, et al. Interaction of oral bacteria with gingival epithelial cell multilayers. Mol Oral Microbiol. 2011;26(3):210–20.
34. Sobue T, et al. Chemotherapy-induced oral mucositis and associated infections in a novel organotypic model. Mol Oral Microbiol. 2018;33(3):212–23.
35. Shang L, et al. Differential influence of Streptococcus mitis on host response to metals in reconstructed human skin and oral mucosa. Contact Dermatitis. 2020;83(5):347–60.
36. Zhang Y, et al. Stable reconstructed human gingiva-microbe interaction model: differential response to commensals and pathogens. Front Cell Infect Microbiol. 2022;12: 991128.
37. Li X, et al. Saliva-derived microcosm biofilms grown on different oral surfaces in vitro. NPJ Biofilms Microbiomes. 2021;7(1):74.
38. Buskermolen JK, et al. Development of a full-thickness human gingiva equivalent constructed from immortalized keratinocytes and fibroblasts. Tissue Eng Part C Methods. 2016;22(8):781–91.

39. Shang L, et al. Multi-species oral biofilm promotes reconstructed human gingiva epithelial barrier function. Sci Rep. 2018;8(1):16061.
40. Shang L, et al. Commensal and pathogenic biofilms alter toll-like receptor signaling in reconstructed human gingiva. Front Cell Infect Microbiol. 2019;9: 282.
41. Buskermolen JK, et al. Saliva-derived commensal and pathogenic biofilms in a human gingiva model. J Dent Res. 2018;97(2):201–8.
42. Janus MM, et al. In vitro phenotypic differentiation towards commensal and pathogenic oral biofilms. Biofouling. 2015;31(6):503–10.
43. Exterkate RA, Crielaard W, Ten Cate JM. Different response to amine fluoride by Streptococcus mutans and polymicrobial biofilms in a novel high-throughput active attachment model. Caries Res. 2010;44(4):372–9.
44. Cieplik F, et al. Microcosm biofilms cultured from different oral niches in periodontitis patients. J Oral Microbiol. 2019;11(1):1551596.
45. Koopman JE, et al. Nitrate and the origin of saliva influence composition and short chain fatty acid production of oral microcosms. Microb Ecol. 2016;72(2):479–92.
46. Kozich JJ, et al. Development of a dual-index sequencing strategy and curation pipeline for analyzing amplicon sequence data on the MiSeq Illumina sequencing platform. Appl Environ Microbiol. 2013;79(17):5112–20.
47. Chen T, et al. The human oral microbiome database: a web accessible resource for investigating oral microbe taxonomic and genomic information. Database (Oxford). 2010;2010:baq013.
48. McMurdie PJ, Holmes S. phyloseq: an R package for reproducible interactive analysis and graphics of microbiome census data. PLoS ONE. 2013;8(4):e61217.
49. Langhorst J, et al. Elevated human beta-defensin-2 levels indicate an activation of the innate immune system in patients with irritable bowel syndrome. Am J Gastroenterol. 2009;104(2):404–10.
50. Spiekstra SW, et al. Induction of cytokine (interleukin-1alpha and tumor necrosis factor-alpha) and chemokine (CCL20, CCL27, and CXCL8) alarm signals after allergen and irritant exposure. Exp Dermatol. 2005;14(2):109–16.
51. Segata N, et al. Metagenomic biomarker discovery and explanation. Genome Biol. 2011;12(6): R60.
52. Wayakanon K, et al. Polymersome-mediated intracellular delivery of antibiotics to treat Porphyromonas gingivalis-infected oral epithelial cells. FASEB J. 2013;27(11):4455–65.
53. Pinnock A, et al. Characterisation and optimisation of organotypic oral mucosal models to study Porphyromonas gingivalis invasion. Microbes Infect. 2014;16(4):310–9.
54. De Ryck T, et al. Development of an oral mucosa model to study host-microbiome interactions during wound healing. Appl Microbiol Biotechnol. 2014;98(15):6831–46.
55. Mark Welch JL, Dewhirst FE, Borisy GG. Biogeography of the oral microbiome: the site-specialist hypothesis. Annu Rev Microbiol. 2019;73:335–58.
56. Eren AM, et al. Oligotyping analysis of the human oral microbiome. Proc Natl Acad Sci U S A. 2014;111(28):E2875–84.
57. Mark Welch JL, Ramirez-Puebla ST, Borisy GG. Oral microbiome geography: micron-scale habitat and niche. Cell Host Microbe. 2020;28(2):160–8.
58. Donati C, et al. Uncovering oral Neisseria tropism and persistence using metagenomic sequencing. Nat Microbiol. 2016;1(7):16070.
59. Shang L, et al. Oral host-microbe interactions investigated in 3D organotypic models. Crit Rev Microbiol. 2024;50(4):397–416.
60. Adelfio M, et al. A physiologically relevant culture platform for long-term studies of in vitro gingival tissue. Acta Biomater. 2023;167:321–34.
61. Silva S, et al. Candida glabrata and Candida albicans co-infection of an in vitro oral epithelium. J Oral Pathol Med. 2011;40(5):421–7.
62. Morse DJ, et al. Denture-associated biofilm infection in three-dimensional oral mucosal tissue models. J Med Microbiol. 2018;67(3):364–75.
63. Pelaez-Prestel HF, et al. Immune tolerance in the oral mucosa. Int J Mol Sci. 2021;22(22):12149.
64. Hajishengallis G, et al. Low-abundance biofilm species orchestrates inflammatory periodontal disease through the commensal microbiota and complement. Cell Host Microbe. 2011;10(5):497–506.
65. Koning JJ, et al. A multi-organ-on-chip approach to investigate how oral exposure to metals can cause systemic toxicity leading to Langerhans cell activation in skin. Front Toxicol. 2021;3: 824825.
66. Kosten IJ, et al. MUTZ-3 Langerhans cell maturation and CXCL12 independent migration in reconstructed human gingiva. Altex. 2016;33(4):423–34.

Publisher's Note